The Calcium Binding Site in Cytochrome aa_3 from *Paracoccus denitrificans*†

Sirpa Riistama, Liisa Laakkonen, Mårten Wikström, Michael I. Verkhovsky, and Anne Puustinen*

Helsinki Bioenergetics Group, Department of Medical Chemistry, Institute of Biomedical Sciences and Biocentrum Helsinki, P.O. Box 8, 00014 University of Helsinki, Helsinki, Finland

Received April 15, 1999; Revised Manuscript Received May 27, 1999

ABSTRACT: A shift in the spectrum of heme *a* induced by calcium or proton binding, or by the proton electrochemical gradient, has been attributed to interaction of Ca^{2+} or H^+ with the vicinity of the heme propionates in mitochondrial cytochrome *c* oxidase, and proposed to be associated with the exit path of proton translocation. However, this shift is absent in cytochrome *c* oxidases from yeast and bacteria [Kirichenko et al. (1998) *FEBS Lett. 423*, 329−333]. Here we report that mutations of Glu56 or Gln63 in a newly described Ca^{2+}/Na^+ binding site in subunit I of cytochrome *c* oxidase from *Paracoccus denitrificans* [Ostermeier et al. (1997) *Proc. Natl. Acad. Sci. U.S.A. 94*, 10547−10553] establish the Ca^{2+}-dependent spectral shift in heme *a*. This shift is counteracted by low pH and by sodium ions, as was described for mammalian cytochrome *c* oxidase, but in the mutant *Paracoccus* enzymes Na^+ is also able to shift the heme *a* spectrum, albeit to a smaller extent. We conclude that the Ca^{2+}-induced shift in both *Paracoccus* and mitochondrial cytochrome aa_3 is due to binding of the cation to the new metal binding site. Comparison of the structures of this site in the two types of enzyme allows rationalization of their different reactivity with cations. Structural analysis and data from site-directed mutagenesis experiments suggest mechanisms by which the cation binding may influence the heme spectrum.

Cytochrome *c* oxidases of mitochondrial or bacterial origin catalyze the reduction of O_2 to water at a bimetallic heme iron (a_3)−copper (Cu_B) center in subunit I of the membrane-bound enzyme. This reaction is coupled to proton translocation across the mitochondrial or bacterial membrane (*1*). Subunit II contains the binuclear Cu_A center, which is the primary acceptor of electrons from cytochrome *c*, and donates electrons to heme *a* in subunit I, from which they are transferred to the O_2 reduction site. The enzyme also contains tightly bound metals that are not redox-active. An Mg^{2+} or Mn^{2+} binding site is close to the heme a_3 propionate groups, and Zn^{2+} is bound to the nuclear-coded subunit Vb in the mitochondrial enzyme (*2*).

Nearly 30 years ago Wikström found that the optical spectrum of ferrocytochrome *a* is red-shifted by 1−2 nm upon "energization" of isolated mitochondria by ATP (see refs *3*−*5*). It was shown subsequently that this spectral shift can be mimicked by calcium ions, which are bound to the enzyme from the positively charged (P) side of the membrane (*6*), and that the latter phenomenon is also seen in isolated cytochrome *c* oxidase. The same spectral change could also be induced by H^+ ions (*7*), and thus proton binding from the P side of the membrane, driven by the electrochemical proton gradient, seemed a plausible explanation for the spectral shift, which was found to be induced by ATP hydrolysis, respiratory activity, or electrical diffusion potential (*8*). The Ca^{2+}-induced shift was reported to be highly specific for this cation (and for H^+), but Mkrtchyan et al. (*9*) found subsequently that it could be reversed or prevented by high concentrations of sodium ions, though Na^+ itself was not capable of inducing the shift. Saari et al. (*7*) showed that an analogous spectral change was induced in isolated bis-imidazole heme A by calcium, though in this case with low cation specificity. This latter effect was prevented by esterification of the propionate groups of heme A, indicating that the effect of Ca^{2+} (and H^+) in situ may be exerted by interaction of the ion with the vicinity of the propionate carboxyl(s) of heme *a*. Due to the sidedness of the calcium effect, it was also concluded that the propionate(s) of heme *a* must be located on the P side of the membrane, not far from the membrane surface. However, the major interest in the calcium-induced effect comes from the finding that it is also caused by proton binding, presumably to the same site, at a high electrochemical proton gradient. Thus, this metal binding site shows the properties and location expected from an acidic site involved in the exit "channel" of the proton pump (*7*).

A new metal binding site was recently reported in the crystal structures of cytochrome *c* oxidase from both *Paracoccus denitrificans* (*10*) and bovine heart mitochondria (*11*) (Figure 1). This site, which was proposed to bind either Ca^{2+} or Na^+ (*10*, *11*), is situated on the P side membrane border of subunit I, and appears well accessible since the other subunits are not blocking it. It is formed by residues on the top of transmembrane helix I of subunit I, and in the loop following it, with possible additional contacts from the loop between transmembrane helices XI and XII. The identity of the ion cannot be definitely determined from the present crystal structures. In *P. denitrificans*, the authors prefer coordination with Ca^{2+} whereas Na^+ is preferred in the structure proposed by Yoshikawa et al. (*11*). In the latter case, Na^+ was reported to fit better to the electron density, assuming that the ion has the same temperature factor as the surrounding residues.

† Supported by grants from the Academy of Finland, the University of Helsinki, and the Sigrid Juselius Foundation.

* To whom correspondence should be addressed. E-mail: Anne.Puustinen@Helsinki.Fi.

10.1021/bi990885v CCC: $18.00
Published on Web 07/27/1999

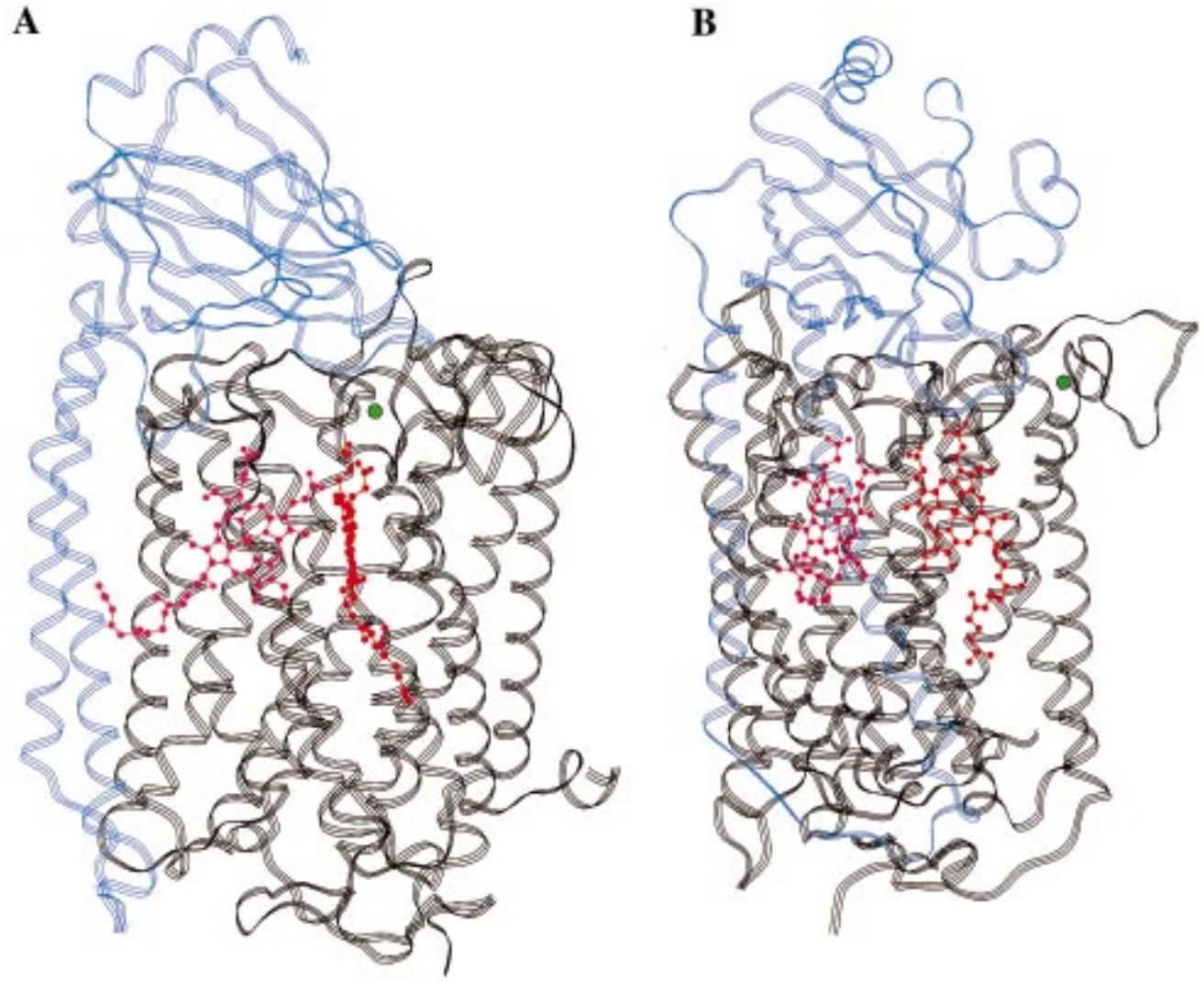

FIGURE 1: Location of the cation binding site in the two-subunit *Paracoccus* cytochrome *c* oxidase. The site is at the end of the transmembrane helix I of subunit I, close to the periplasmic membrane surface. Subunits III and IV (not shown) would be located on the opposite side of the enzyme relative to the metal binding site. (A) Shows the positions of subunits I (black) and II (blue) and hemes (heme *a* in bright red on the right and heme a_3 in pink on the left) in the membrane. (B) A view of the Ca^{2+}/Na^+ site (green dot) close to the protein surface.

Kirichenko et al. (*12*) recently suggested that the Ca^{2+}-induced shift in heme *a* is the result of binding of the cation to this newly described metal binding site, but no experimental evidence for this suggestion is available. These authors reported that the Ca^{2+}-induced shift is absent in cytochrome *c* oxidases from bacteria and yeast, and proposed that this specificity is due to interaction of Ca^{2+} with species-specific ligands that account for the perturbation of heme *a* in the mammalian enzyme. Since the metal binding site is nevertheless quite similar structurally in the bacterial and mammalian cytochrome *c* oxidases, we undertook a site-directed mutagenesis study of it in the *Paracoccus* enzyme to explore whether it can be modified to exhibit the Ca^{2+}-dependent spectral change. In the absence of such direct evidence, this site cannot be assigned as the one specifically responsible for the cation-induced spectral shift.

MATERIALS AND METHODS

Site-Directed Mutagenesis. The system for in vitro mutagenesis is based on the method by Vandeyar et al. (*13*). A 1.8 kb *Xba*I−*Hin*dIII or a 1.6 kb *Pst*I−*Hin*dIII fragment containing the *cta*DII gene encoding subunit I (*14*) was moved into M13mp18 and used as a template. After mutagenesis, the mutants were cloned into a derivative of the broad-host strain plasmid pBBR1MCS (*15*) containing a streptomycin marker (*16*), the *cta*DII gene, and its promoter region. The *E. coli* strain SM10 transformed with this expression plasmid was allowed to conjugate with *P. denitrificans* strain AO1, from which the chromosomal copies of the *cta*DII and its isogene *cta*DI are deleted, and where the ccoN gene, which encodes subunit I of the alternative cbb_3 cytochrome oxidase, is inactivated (*16*). Mutations were confirmed by DNA sequencing (ALFexpress DNA sequencer, Pharmacia) throughout all processing stages, as well as from fermentor cultivations.

Bacterial Growth and Enzyme Purification. Wild-type and mutant strains of *P. denitrificans* were grown at 32 °C under strong aeration in a 30 L fermentor using succinate (50 mM) as carbon source in the minimal medium (*17*) that was not supplemented by extra Ca^{2+}. Streptomycin (25 μg/mL) was also used in fermentor cultivations. Cells were harvested in the exponential growth phase, and the yield was ~50 g of cells/25 L.

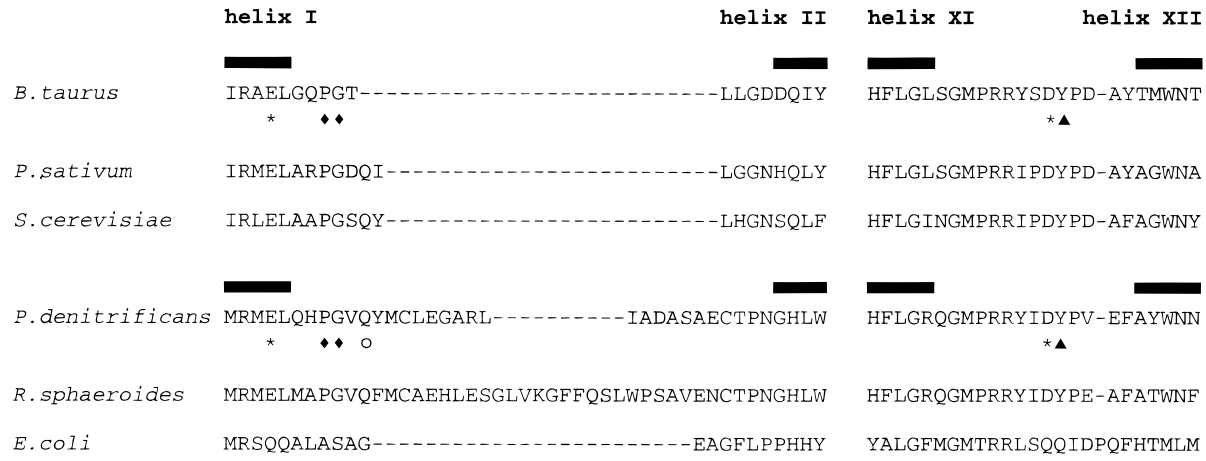

FIGURE 2: Protein sequence alignment of the two sides of the metal binding site in mammalian, yeast, and bacterial cytochrome *c* oxidase. The ends and beginnings of the transmembrane helices (black bars) and the loops between them forming the pocket are shown. Amino acids involved in the ligation of metal are also marked: carboxylic acids Glu56 and Asp477 in *Paracoccus* (Glu40 and Asp442 in bovine enzyme) (∗); the conformationally important proline 60 and glycine 61 in *Paracoccus* (Pro44 and Gly45 in bovine enzyme) (♦); tyrosine 478 in *Paracoccus* (Tyr443 in bovine enzyme) (▲); and glutamine 63 in *Paracoccus* (○).

Bacterial membranes were prepared by lysozyme treatment and osmotic lysis of cells (*18*). The level of expression of cytochrome *c* oxidase in these membranes was insufficient for spectroscopic experiments. To isolate the enzyme, salt-washed membranes were solubilized with 1% (w/v) dodecyl maltoside (DM)(Anatrace) in 20 mM Tris-HCl, pH 7.8, 0.2 mM PMSF. After ultracentrifugation, the supernatant was applied to a DEAE-Sepharose FF (Pharmacia) column equilibrated with 50 mM NaCl, 20 mM Tris-HCl, pH 7.8, 0.5 mM EDTA, and 0.025% DM. Elution of cytochrome aa_3 was done with a 50−300 mM NaCl gradient in 0.05% DM, 20 mM Tris-HCl, pH 7.8, 0.5 mM EDTA. The cytochrome aa_3-containing fractions were pooled and concentrated using pressure dialysis (Amicon, YM-100 membrane), and diluted to lower the Na^+ concentration before the second column [Q-Sepharose FF (Pharmacia)], which had been equilibrated with 100 mM NaCl, 0.05% DM, 20 mM Tris-HCl, pH 7.8, 0.5 mM EDTA. The enzyme was eluted at the end of the NaCl gradient (10× bed volume) from 100 to 400 mM. After SDS−PAGE analysis, fractions containing pure three-subunit cytochrome aa_3 were pooled and concentrated as above, and finally using Centricon-50 concentrators (Amicon).

Activity Measurements. Oxygen consumption was measured using a Clark-type oxygen electrode. The reaction medium was 50 mM phosphate buffer, pH 6.5, supplemented with 0.05% DM, 2.9 mM ascorbate, 34 μM horse heart cytochrome *c* (Sigma, type VI), 0.6 mM TMPD, and 1.1 mg/mL asolectin. The rate of oxygen uptake was determined after addition of enzyme.

Proton Translocation. Spheroplast treatment of the *P. denitrificans* cells and the oxidant−pulse method used to measure proton translocation were as described previously (*19*). The reaction medium contained either 100 mM KSCN, 100 mM KCl, 100 mM sucrose, and 3 mM $MgCl_2$, or 200 mM KCl, 100 mM sucrose, 3 mM $MgCl_2$, and 0.5−1 μM valinomycin, supplemented with 10−20 μM rotenone and 2.5 mM succinate.

Spectrophotometry. For the cation-induced spectral shift measurements, the enzyme preparations were diluted in 0.05% DM, 20 mM Tris-HCl, pH 7.8, and concentrated again to minimize the Na^+ content. Optical spectra were recorded with a Shimadzu UV-3000 spectrophotometer, which has been updated with a computer connection. Concentrations of cytochrome aa_3 preparations were determined spectrophotometrically from reduced minus oxidized difference spectra using the $\Delta\epsilon(605-630)$ of 23.4 cm^{-1} mM^{-1} (*20*).

The Ca^{2+}-induced spectral shift was measured in 50 mM Bis-tris-propane (BTP; pH 8), 0.5 mM EGTA, 0.02% DM, supplemented with 1 mM KCN, 1 μM cytochrome *c*, 10 μM TMPD, and 4 mM ascorbate. The final enzyme concentration was adjusted to 1.5 μM, except for the cation concentration dependence measurements, in which case it was 3 μM. In the latter case, the background sodium concentration was ca. 0.15 mM, as measured by flame photometry (*21*). The base line spectrum was recorded in the presence of EGTA after which 2 mM $CaCl_2$ or NaCl was added to measure the difference spectrum. Hyperbolic curve-fittings to determine the apparent dissociation constants for Ca^{2+} and Na^+ binding were done with Microcal Origin 4.0 (Microcal Software, Inc.).

Computations and Modeling. Positions of helices in the cytochrome *c* oxidase of *Paracoccus* and bovine heart mitochondria marked in the protein sequence alignment (Figure 2) were defined by the Kabsch−Sander algorithm (*22*) as implemented in Insight II (Version 97.0 Molecular Modeling System, Molecular Modeling Simulations Inc., 1997), and the sequences are aligned using ClustalW 1.74 (*23*). The protein database search was done with the program BLAST (*24*) from the sequence databases Swissprot (*25*) and Genbank (*26*). Ca^{2+} was built into the bovine heart mitochondrial cytochrome aa_3 structure (*11*) with the program Insight II, and the structure was refined by energy optimization using the program CHARMM (*27*). The available Ca^{2+}-bound structure for the *Paracoccus* enzyme (*10*) as well as both structures without bound metal in the site were energy-minimized analogously.

[1] Abbreviations: BTP, Bis-tris-propane; TMPD, *N*,*N*,*N*′,*N*′-tetramethyl-1,4-phenylenediamine; DM, *n*-dodecyl β-D-maltoside; PMSF, phenylmethylsulfonyl fluoride; kb, kilobase pair(s).

RESULTS AND DISCUSSION

According to the report by Ostermeier et al. (*10*), there are five metal binding ligands in the newly described metal binding site of cytochrome *c* oxidase from *Paracoccus*. These are the backbone carbonyl oxygen atoms from residues Glu56, His59, and Gly61, as well as side chain oxygens from Glu56 and Gln63. Based on sequence alignment (Figure 2), the first three residues correspond to Glu40, Gln43, and Gly45 in the bovine enzyme, of which, however, only Glu40 and Gly45 were reported to be metal ligands (*11*). To better understand the structural differences between the sites in the *Paracoccus* and bovine enzymes, Ca^{2+} was built into the bovine enzyme structure, which was then energy-optimized (Figure 3A). The *Paracoccus* site was treated similarily for comparison (Figure 3B). The calcium−oxygen distances found are comparable to the distances of 2.35 ± 0.4 Å reported for calcium sites of various proteins (*28*, *29*). The number of Ca^{2+} ligands in known structures varies greatly, but the most common complexes have 5−8 oxygenous ligands. In addition to the metal ligands reported by Yoshikawa et al. (*11*) for the bovine enzyme, the backbone oxygen of Gln43 forms a good bond to calcium by analogy to a histidine ligand (*10*) in the corresponding position of the *Paracoccus* enzyme (cf. above). In addition, the side chain oxygens from Asp442 and Tyr443 also form bonds to the metal (Figure 3A). In the *Paracoccus* site (Figure 3B), we found a good bond to calcium from the carboxylic oxygen of Asp477, which is analogous to Asp442 in the bovine enzyme, in addition to the ligands reported by Ostermeier et al. (*10*). This analysis shows that Ca^{2+} can be coordinated electroneutraly to the site with two counter-charges from side chain carboxyls of homologous glutamic and aspartic acids in both the *Paracoccus* and bovine structures.

One obvious difference between the metal binding sites is the side chain interaction by Gln63 in *Paracoccus* (Figure 3B), which is missing in the bovine enzyme. Gln63 seems to protect the metal site against the exterior of the subunit, thus possibly blocking easy dissociation of the cation from the site. Interestingly, this residue is also found in the cytochrome *c* oxidases from *S. cerevisiae* and *R. sphaeroides* (Figure 2), which lack the Ca^{2+}-induced spectral shift (*12*). On this basis, Gln63 was mutated into an alanine. We first confirmed that Ca^{2+} does not shift the spectrum of reduced heme *a* in the wild-type *Paracoccus* enzyme (Figure 4; ref *12*). However, the Gln63Ala mutant enzyme does exhibit a Ca^{2+}-induced red shift, although its amplitude in the α-band difference spectrum is only 30% of that in the bovine enzyme (Figure 4).

Amino acid substitutions were also done to the conserved residue Glu56, which provides a side chain as well as a backbone interaction with the metal in the cytochrome *c* oxidases (Figure 3). In the most conservative mutation, Glu56Asp, the spectral shift is very small or absent, but in the mutants Glu56Gln and Glu56Ala it is clearly observed with amplitudes approaching 60% of the shift in the bovine enzyme (Figure 4). Oxygen consumption and proton translocation activities were normal in all mutant enzymes, indicating that the effect of amino acid substitutions is restricted to the metal binding site.

Titration of the Ca^{2+}-induced spectral shift in the Glu56Gln mutant enzyme revealed a K_d of approximately 100 μM for this cation (Figure 5A), which is much higher than the reported K_d of 1.3 μM for the bovine enzyme (*12*). Another difference is that Na^+ itself also causes a qualitatively identical spectral shift in this mutant, with an apparent K_d of 270 μM (Figure 5B). Much higher concentrations of Na^+ are needed to counteract the Ca^{2+}-induced shift in the bovine enzyme, and in that case Na^+ causes no shift on its own (*9*, *12*). In the Glu56Gln mutant enzyme, the maximum amplitude of the Na^+-induced shift was about half of the maximum shift caused by Ca^{2+}. If Na^+ was added first at a concentra-

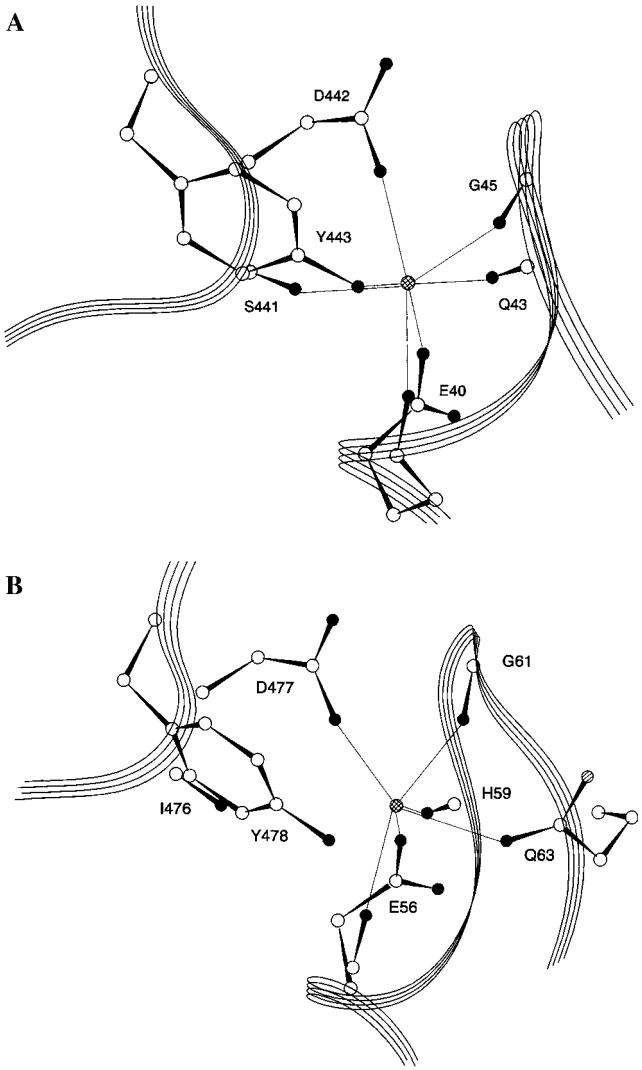

FIGURE 3: Energy-minimized Ca^{2+} binding site in (A) bovine heart mitochondria cytochrome *c* oxidase and (B) *Paracoccus* cytochrome *c* oxidase. The two main structures of the binding pocket are shown (see text). The ribbon shows the path of the protein backbone, and amino acids involved in the binding of metal are marked. Atoms are marked as spheres: carbons (white), oxygens (black), nitrogens (hatched), and calcium (cross-hatched sphere). (A) Thin lines mark the seven interactions found for the bovine enzyme. The backbone and side chain oxygens of Glu40 at 2.49 and 2.47 Å and the backbone oxygens of Gly45 (2.46 Å) and Ser441 (2.31 Å) were described as ligands by Yoshikawa et al. (*11*). In addition, the side chain oxygens from Asp442 (2.34 Å) and Tyr443 (2.73 Å) and the backbone oxygen of Gln43 (2.33 Å) are ligated to calcium. (B) In the *Paracoccus* structure, there are six ligand contacts between the bound Ca^{2+} and residues around it. These are the backbone and side chain oxygens of Glu56 (2.46 and 2.31 Å), the backbone oxygens of His59 (2.49 Å) and Gly61 (2.41 Å), and the side chain oxygen of Gln63 (2.45 Å), as reported by Ostermeier et al. (*10*), *plus* a bond from the carboxylic oxygen of Asp477 (2.31 Å).

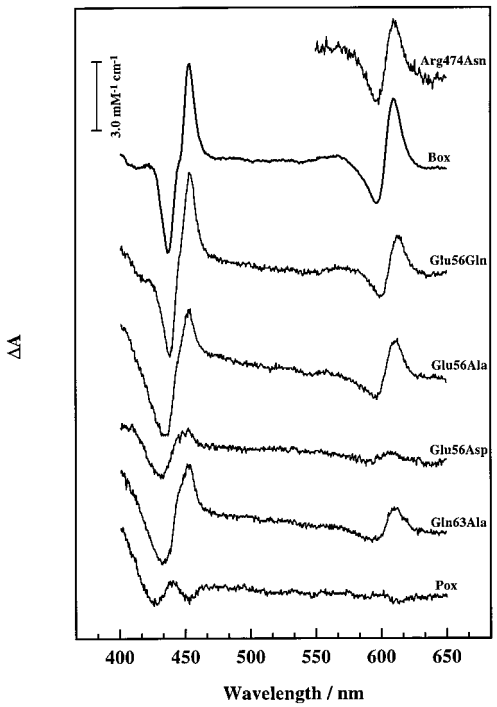

FIGURE 4: Effects of Ca^{2+} on the absorption spectra of reduced heme *a* of cytochrome *c* oxidases from bovine heart mitochondria (Box), from wild-type *Paracoccus* (Pox), and from the mutants Glu56Gln, Glu56Ala, Glu56Asp, and Gln63Ala were determined as described under Materials and Methods using 1.5 μM enzyme. The difference spectrum of reduced minus oxidized heme *a* in the α-region for the wild-type enzyme versus Arg474Asn mutant enzyme is also shown.

tion of 6.5 mM to saturate the Na^+-induced shift, further addition of Ca^{2+} induced the remaining half of the total calcium shift, although then with the K_d apparently raised to 1.5 mM (Figure 5C). This nonadditivity of the effects of the two ions and the Na^+-induced apparent increase in K_d for Ca^{2+} both indicate that Ca^{2+} and Na^+ compete with each other for binding to the same site in the mutant enzyme, and that the effect on heme *a* is caused by a similar mechanism. The ion specificity of the Ca^{2+}-induced shift in the Glu56Gln mutant was also tested with high concentrations of Li^+, K^+, Mg^{2+}, and Mn^{2+} (not shown), which all reduced the effect of Ca^{2+}, though none of them induced the spectral shift themselves. Of these, Li^+ was the most effective, reducing the amplitude of the Ca^{2+}-induced shift to 30% at 50 mM. This is in contrast to high cation specificity found with the mitochondrial enzyme.

Figure 6 shows that the extent of the Ca^{2+}-induced spectral shift in the Glu56Gln mutant depends on pH. As observed earlier for the mammalian enzyme (*7*), the shift is reduced at lower pH; the half-maximal effect is achieved at pH 6.6, which is 0.5−1 pH unit more alkaline than the reported p*K* values for the bovine enzyme (*7*, *12*).

We conclude that the cation binding site found by X-ray crystallography in the cytochrome *c* oxidase structure (*10*, *11*) is indeed the site through which binding of Ca^{2+} (or Na^+ or H^+) perturbs the spectrum of heme *a*. The chemical identity of the cation in the native enzymes is not known from the present crystal structures, nor under physiological conditions. Our data suggest that it may be Na^+ in the native *Paracoccus* enzyme used in this study, because the spectrum of reduced minus oxidized heme *a* of the Gln63Ala and

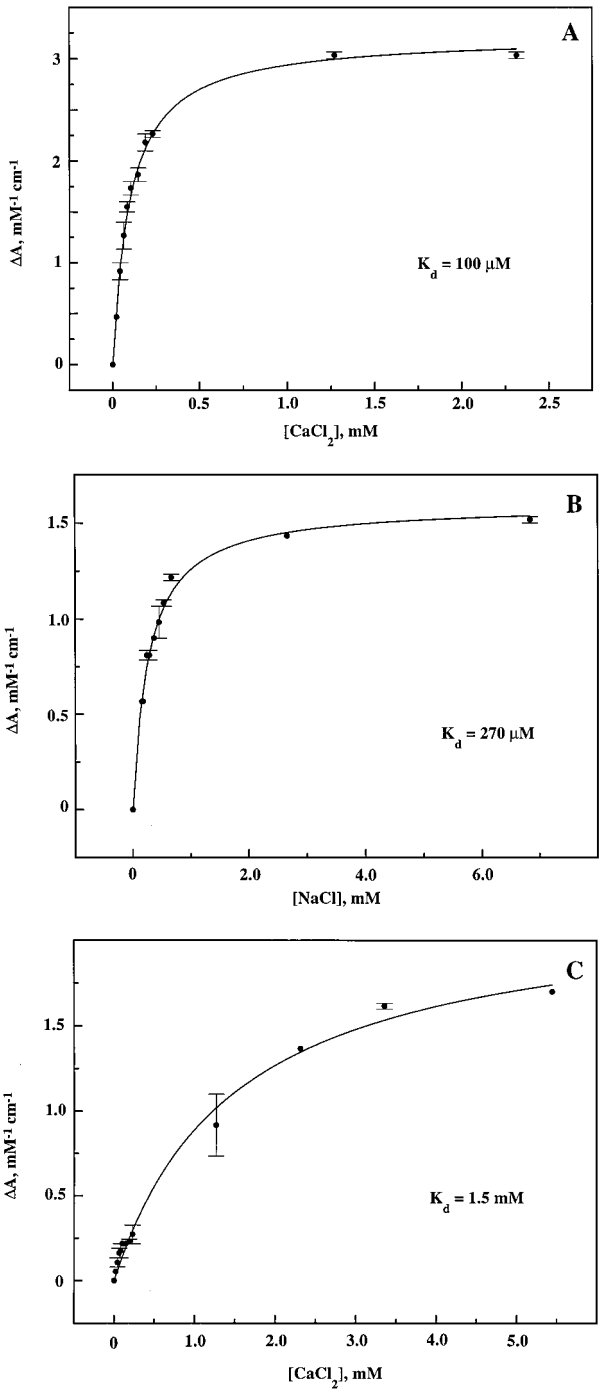

FIGURE 5: Concentration dependence of the Ca^{2+}- and Na^+-induced spectral shift in the Glu56Gln mutant enzyme. 3 μM Glu56Gln mutant enzyme was titrated as described under Materials and Methods. The size of the Ca^{2+}- or Na^+-induced spectral shift was calculated from the absorbance difference between the wavelength pair 599/612 nm. The data were fitted with a hyberbolic curve to calculate the apparent K_d value. (A) Dependence of the spectral shift on $[Ca^{2+}]$. (B) Dependence of the spectral shift on $[Na^+]$; the background of 0.15 mM Na^+ has been subtracted. (C) Dependence of the spectral shift on $[Ca^{2+}]$ in the presence of 6.5 mM NaCl.

Glu56Ala mutant enzymes without cation added is shifted to the blue relative to wild type, and Ca^{2+} shifts the heme spectrum in these mutants to the red, beyond the position of the wild-type spectrum (not shown).

In the *Paracoccus* structure, there is a unique insertion after the metal ligands at the top of the transmembrane helix I and in the loop following it (Figures 1 and 2). The structural

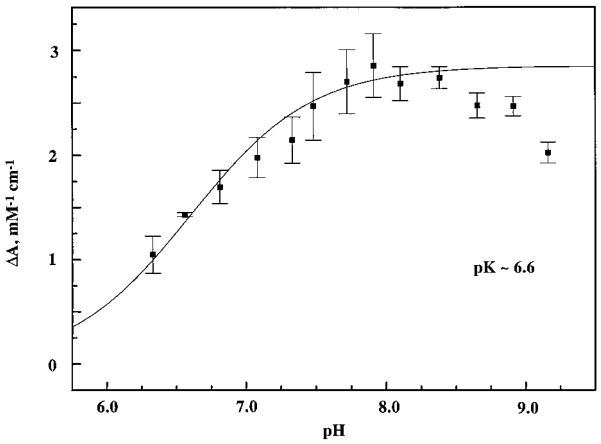

FIGURE 6: Effect of pH on the Ca^{2+}-induced spectral shift in the Glu56Gln mutant oxidase. The extent of the Ca^{2+}-induced spectral shift in the α-band was measured as described under Materials and Methods by varying the pH of 50 mM BTP buffer. The p*K* value was found to be around 6.6. The mean values of three different measurements with standard deviations are shown.

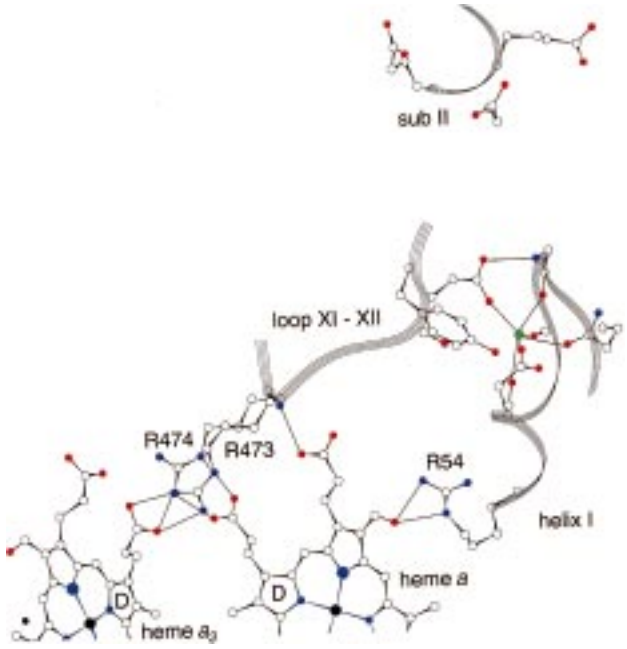

FIGURE 7: Two possible paths for interaction between the Ca^{2+}/Na^+ binding site and heme *a* in *Paracoccus* cytochrome *c* oxidase. The spectral shift induced by cations could be through the loop between helices XI−XII containing arginines 473 and 474, which interact with the propionates of hemes *a* and a_3. The observed effect might also be mediated via the formyl group of heme *a*, which forms a hydrogen bond to the Arg54 in helix I. The protein backbone is marked with ribbons and carbons with empty black spheres, oxygens are red and nitrogens are blue spheres, and calcium is the green sphere.

importance of this insertion for the metal binding site is probably small, because it is restrained by a disulfide bridge between two cysteine residues found at each end of the insertion. The overall fold of the loop that contains most of the metal ligands is very similar in both structures. Transmembrane helix I ends at the same point, and the conformationally important proline 60 and glycine 61 in *Paracoccus* (44 and 45 in bovine) are conserved (Figure 2). It is noteworthy that this glycine has dihedral angles (ϕ, ψ) of 132.42° and −171.08° for the bovine, and 91.51° and 130.93° for the *Paracoccus* enzyme, so that it cannot be replaced with other residues without changing the folding of the peptide backbone. Another structural restriction is caused by the interaction of the backbone nitrogen of this glycine with the side chain of an aspartic acid (477 in *Paracoccus* enzyme; 442 in bovine enzyme) in the loop between helices XI and XII (Figures 3, 7). In the energy-minimized *Paracoccus* structure, the lengths of the hydrogen bonds between the amino N of Gly61 and the carboxyl oxygens of Asp477 are 2.83 and 2.55 Å. In the bovine structure, the corresponding distances are longer (3.31 and 3.33 Å), most likely because the aspartic acid can also form a hydrogen bond with an arginine (Arg134) in subunit II. This latter interaction is absent from *Paracoccus* cytochrome oxidase, and could be one of the structural differences between the bovine and *Paracoccus* enzymes responsible for the observed differences in the Ca^{2+}-induced spectral change.

The metal binding pocket is formed by two main structures, viz., the top of transmembrane helix I with the loop following it, and by the loop between helices XI and XII (Figures 2, 7). Binding of calcium to the pocket could bridge these two sides of the binding site together, and thus induce a conformational change in either or both of these structures, which may cause the spectral shift in the optical absorption spectrum of heme *a*. In the bovine enzyme, Na^+ does not cause a spectral red shift by itself, but can reverse the shift caused by Ca^{2+}, while Na^+ does induce a spectral shift in the present *Paracoccus* mutants, albeit smaller than that with Ca^{2+}. These cations most likely bind to the same site, but do not achieve identical effects. In *Paracoccus*, the top of the Ca^{2+} binding pocket is not connected to subunit II and the hydrogen bonds between Gly61 and Asp477 are strong and stable throughout the molecular dynamic simulations (Figures 3B and 7), and the structure of the site is not affected by Ca^{2+}. Therefore, it seems that the metal binding pocket in *Paracoccus* is so well organized that also a monovalent cation can contact both sides. In contrast, in the bovine enzyme the pocket is more mobile, and hydrogen bonds between Gly45 and Asp442 are only found in the structure with bound Ca^{2+}, but not if the binding site is empty. In this situation, Na^+ alone may not be able to induce the structural changes needed for the spectral shift (see below).

The loop between transmembrane helices XI and XII contains conserved arginines (Figure 7), which interact with the propionates of hemes *a* and a_3 (473 and 474 in *Paracoccus* enzyme; 438 and 439 in bovine enzyme). Of these, Arg474 is closer to the ring D propionate of heme *a*, whereas Arg473 is closer to the D propionate of heme a_3. A change in the helix XI−XII loop may be felt by heme *a* if, for example, it causes Arg474 to move further toward the ring D propionate of heme *a*, strengthening the hydrogen bonding. If the effect is indeed exerted via a propionate group of heme *a*, as suggested by Saari et al. (*7*), it is likely to be electrostatic in nature because the propionates are not conjugated to the heme macrocycle. The Arg474−propionate interaction is, in part, electrostatic (*30*), but Arg474 also donates a hydrogen bond from Nϵ to the carboxyl oxygen of the propionate (*10*). We tested this possibility by mutating Arg474 to an asparagine. As shown in Figure 4, this mutation causes a blue shift in the spectrum of ferrous heme *a*, which is similar in position, and only some 25% larger in amplitude, when compared to the Ca^{2+}-induced shift in the Glu56Gln

mutant enzyme. This finding indicates that the positively charged Arg474 indeed influences the spectrum of heme *a*, shifting it to the red in much the same way as does Ca^{2+}. It is noteworthy that this mutation has no effect on the proton translocation efficiency of the enzyme (cf. *31*), and that the catalytic activity is not much changed (not shown).

Another possible mechanism for the Ca^{2+}-induced spectral shift involves interaction with the macrocycle of heme *a* via the conjugated formyl group. As pointed out by Babcock and Callahan (*32*), the optical spectrum of heme *a* is considerably red-shifted in aa_3-type cytochrome *c* oxidases relative to heme A model compounds. They considered that hydrogen bonding between the formyl group in position 8 of the heme and a residue in the protein may be responsible for this shift, and evidence for such a mechanism was obtained from resonance Raman studies of cytochrome *c* oxidases and heme A model compounds. The extent of a red shift of this kind in the optical spectrum is expected to depend on the strength (i.e., of distance and angle) of such a hydrogen bond—the stronger the bond, the more extensive the spectral shift to the red. A conserved arginine (54 in the *Paracoccus* enzyme; 38 in the bovine enzyme) is within hydrogen-bonding distance to the formyl group of heme *a* (*10*, *11*), and could thus cause the red shift in the spectrum. This arginine is positioned in transmembrane helix I, and is indeed close to the Glu56 ligand of the cation binding site (Figure 7). A Ca^{2+}-induced change in the conformation of helix I, as discussed above, could shorten the distance between the nitrogen atom of Arg54 and the oxygen atom of the heme *a* formyl group, and/or make a hydrogen bond between them more linear. In both cases, strengthening of the hydrogen-bonding interaction would be expected to shift the heme *a* spectrum to the red. Mutation of Arg54 alone, and/or together with residues in the metal binding site, could give more information about the validity of this latter mechanism.

CONCLUSIONS

Our data indicate that the spectral change in heme *a* (*3*−*9*) caused by Ca^{2+} (or Na^+ or H^+) is due to binding of these cations to the newly described metal binding site in cytochrome *c* oxidase (*10*, *11*). This spectral change, which does not occur in the wild-type *Paracoccus* enzyme (*12*), can be induced by mutations within the binding site. Two major differences between the bovine and wild-type *Paracoccus* enzyme structures may account for the difference in their reactivity toward Ca^{2+}. A glutamine ligand (Gln63) in the *Paracoccus* structure appears to shield the site, and hydrogen bonding between Gly61 and the carboxyl oxygens of Asp477 may stabilize it relative to the bovine enzyme. Thus, a cation bound to the wild-type *Paracoccus* site may not be easily dissociable. Analysis of the structures of the bovine and *Paracoccus* enzymes suggests that the spectral change may be due to a change in the organization of the interhelical loops I−II and XI−XII, which are parts of the cation binding site. Two plausible mechanisms for the spectral change emerge from this analysis, viz., perturbation of the vicinity of ring D propionate of heme *a*, which is supported by the effect of mutating the nearby arginine 474 in loop XI−XII, and perturbation of the interaction between the formyl group of heme *a* and a nearby arginine in helix I, which is supported by earlier resonance Raman data (*32*).

The structural and functional role of the metal binding site remains obscure, however. It seems to be absent from the quinol oxidases, and its role might therefore be connected to electron transfer from cytochrome *c* via the Cu_A center into the low-spin heme. Alternatively, it might help to regulate proton translocation events. Proton translocation is known to be less tightly coupled to the O_2 reduction chemistry in the bo_3-type quinol oxidase from *E. coli* (*33*), which lacks the metal binding site.

ACKNOWLEDGMENT

We are grateful to Drs. O.-M. H. Richter and B. Ludwig for the streptomycin derivative of plasmid pBBR1MSC and the strain AO1, and to Eija Haasanen for excellent technical assistance.

REFERENCES

1. Babcock, G. T., and Wikström, M. (1992) *Nature 356*, 301−309.
2. Tsukihara, T., Aoyama, H., Yamashita, E., Tomizaki, T., Yamaguchi, H., Shinzawa-Itoh, K., Nakashima, R., Yaono, R., and Yoshikawa, S. (1995) *Science 269*, 1069−1074.
3. Wikström, M. K. F., and Saris, N. E. L. (1970) in *Electron Transport and Energy Conservation* (Tager, J. M., Papa, S., Quagliariello, E., and Slater, E. C., Eds.) pp 77−88, Adriatica Editrice, Bari, Italy.
4. Wikström, M. K. F. (1972) *Biochim. Biophys. Acta 283*, 385−390.
5. Wikström, M. K. F. (1974) *Ann. N.Y. Acad. Sci. 227*, 146−158.
6. Wikström, M. K. F., and Saari, H. (1975) *Biochim. Biophys. Acta 408*, 170−179.
7. Saari, H., Penttilä, T., and Wikström, M. (1980) *J. Bioenerg. Biomembr. 12*, 325−338.
8. Wikström, M. K. F., and Saari, H. (1976) *Mol. Cell. Biochem. 11*, 17−33.
9. Mkrtchyan, H., Vygodina, T., and Konstantinov, A. (1990) *Biochem. Int. 20*, 183−190.
10. Ostermeier, C., Harrenga, A., Ermler, U., and Michel, H. (1997) *Proc. Natl. Acad. Sci. U.S.A. 94*, 10547−10553.
11. Yoshikawa, S., Shinzawa-Itoh, K., Nakashima, R., Yaono, R., Yamashita, E., Inoue, N., Yao, M., Jie Fei, M., Peters Libeu, C., Mizushima, T., Yamaguchi, H., Tomizaki, T., and Tsukihara, T. (1998) *Science 280*, 1723−1729.
12. Kirichenko, A., Vygodina, T., Mkrtchyan, H. M., and Konstantinov, A. (1998) *FEBS Lett. 423*, 329−333.
13. Vandeyar, M., Weiner, M., Hutton, C., and Batt, C. (1988) *Gene 65*, 129−133.
14. Raitio, M., Pispa, J. M., Metso, T., and Saraste, M. (1990) *FEBS Lett. 261*, 431−435.
15. Kovach, M. E., Phillips, R. W., Elzer, P. H., Roop, R. M., and Peterson, K. M. (1994) *BioTechniques 16*, 800−802.
16. Pfitzner, U., Odenwald, A., Ostermann, T., Weingard, L., Ludwig, B., and Richter, O.-M. H. (1998) *J. Bioenerg. Biomembr. 30*, 89−97.
17. Chang, J. P., and Morris, J. G. (1962) *J. Gen. Microbiol. 29*, 301−310.
18. Berry, E. A., and Trumpower, B. L. (1985) *J. Biol. Chem. 260*, 2458−2467.
19. Puustinen, A., Finel, M., Virkki, M., and Wikström, M. (1989) *FEBS Lett. 249*, 163−167.
20. Ludwig, B., and Schatz, G. (1980) *Proc. Natl. Acad. Sci. U.S.A. 77*, 196−200.
21. Verkhovskaya, M. L., Verkhovsky, M. I., and Wikström, M. (1996) *FEBS Lett. 388*, 217−218.
22. Kabsch, W., and Sander, C. (1983) *Biopolymers 22*, 2577−2637.

23. Thompson, J. D., Higgins, D. G., and Gibson, T. J. (1994) *Nucleic Acids Res. 22*, 4673−4680.
24. Altschul, S. F., Madden, T. L., Schäffer, A. A., Zhang, J., Zhang, Z., Miller, W., and Lipman D. J. (1997) *Nucleic Acids Res. 25*, 3389−3402.
25. Bairoch, A., and Apweiler, R. (1999) *Nucleic Acids Res. 27*, 49−54.
26. Benson, D. A., Boguski, M. S., Lipman, D. J., Ostell, J., and Ouellette, B. F. (1998) *Nucleic Acids Res. 26*, 1−7.
27. Brooks, B. R., Bruccoleri, R. E., Olafson, B. D., States, D. J., Swaminathan, S., and Karplus, M. (1983) *J. Comput. Chem. 4*, 187−217.
28. Abola, E. E., Sussman, J. L., Prilusky, J., and Manning, N. O. (1997) *Methods Enzymol. 277*, 556−571.
29. Sussman, J. L., Lin, D., Jiang, J., Manning, N. O., Prilusky, J., Ritter, O., and Abola, E. E. (1998) *Acta Crystallogr. D54*, 1078−1084.
30. Kannt, A., Lancaster, C. R. D., and Michel, H. (1998) *Biophys. J. 74*, 708−721.
31. Puustinen, A., and Wikström, M. (1999) *Proc. Natl. Acad. Sci. U.S.A. 96*, 35−37.
32. Babcock, G. T., and Callahan, P. M. (1983) *Biochemistry 22*, 2314−2319.
33. Verkhovskaya, M., Verkhovsky, M., and Wikström, M. (1992) *J. Biol. Chem. 267*, 14559−14562.

BI990885V